Journal of Fluorescence
https://doi.org/10.1007/s10895-023-03325-w

RESEARCH

Fluorescence Study of Pr^{3+} Doped CdS Nanoparticles and its Applications in Sensors and Detectors

Jitendra Pal Singh[1] · **Yogesh Kumar Sharma**[2] · **Sudha Pal**[3] · **Atanu Nag**[1]

Received: 14 April 2023 / Accepted: 20 June 2023

Abstract

Fluorescence spectra of Pr^{3+} doped CdS nanoparticles, synthesized by chemical precipitation method, have been recorded at room temperature. The synthesized particles are nearly spherical shaped and the grain size is decreased with the increase in Pr^{3+} concentration. The chemical identity of the nanoparticles was confirmed by EDAX spectrum, the absorption peaks was confirmed by FTIR spectrum and then the recorded values were compared with the CIE diagram. The oscillator strengths of the 4f ↔ 4I transitions are parameterized in terms of three phenomenological Judd-Ofelt intensity parameters Ω_λ ($\lambda =$ 2, 4 and 6). Using the fluorescence data and these Ω_λ parameters, theoretical and experimental study of various radiative properties viz., spontaneous emission probability (A), radiative life time (τ), fluorescence branching ratio (β) and stimulated emission cross-section(σ_p)were evaluated. The values of these parameters indicate that $^3P_0 \rightarrow {}^3H_4$ transition can be considered to be good laser transition in the visible colour region. Also, excitation with 493 nm, leads to similar blue regions. The synthesized Pr^{3+} doped CdS nanomaterials could be useful for sensing and detecting devices, particularly for temperature sensing measurement and bio-sensing detection.

Keywords Nanoparticles · Fluorescence spectra · Judd-Ofelt parameters · CIE chromaticity diagram

Introduction

Cadmium Sulphide (CdS) has large band gap energy of 2.42 eV at room temperature that enables its nanoparticles to be remarkable in optoelectronics, photonics and photovoltaics. CdS nanoparticles have given much attention for their potential application in future optoelectronic devices due to tunable direct electronic band gap, high absorption co-efficient, good emission efficiency, high thermal stability and easy to be synthesized. CdS nanoparticles can display novel chemical, electronic, magnetic, optical, structural properties that might find many important technological applications. CdS nanoparticles, due to their good thermal stability, are also used as pigment in paints and in engineered plastic [1]. These particles can be used in optoelectronics for making photocells, light emitting diode (LED), lasers, field effect transistor (FET) etc. [2, 3]. In photonics, due to the photoconducting and electrical properties it can be used in sensors, photo-detectors, optical filters, and optical switches. As its band gap appears in the visible spectrum [4], this is useful for many commercial and potential applications in photovoltaics, as hetero-junction solar cells and thin film solar cells. In photo-catalysis, owing to its photo-chemicals and catalytic properties, CdS nanoparticles can be used for water splitting as well as for water and air purification [5, 6].

In this work, we have synthesized and developed stable and strong Pr^{3+} doped CdS nanomaterials of different concentrations by the simple chemical precipitation method. In present study, the spectral characterization *i.e.*, absorption

✉ Yogesh Kumar Sharma
dryksharma@yahoo.com

Jitendra Pal Singh
paljitendra124@gmail.com

Sudha Pal
palsudh2011@gmail.com

Atanu Nag
tnnag79@gmail.com

[1] Department of Physics, School of Sciences, IFTM University, Moradabad 244001, India

[2] Department of Physics, Pt. L.M.S. Sri Dev Suman Uttarakhand University Campus, Rishikesh (Dehradun), Uttarakhand 249201, India

[3] Department of Physics, M.B. Govt. P.G. College, Haldwani, Uttrakhand 263139, India

and fluorescence (FL) spectra of Pr^{3+} doped CdS nanomaterials have been extensively studied. Having some more attractive features, FL spectroscopy is 2-3 orders of magnitude better than absorption spectroscopy in which even a single molecule can be detected and also phosphorescence is always applicable at longer wavelength compared with fluorescence. The excitement of atoms by absorption of radiation and their return back to the ground state by giving up the excess energy as photons are clearly studied by FL spectroscopy. It can be used as an important technique for measuring the purity and crystalline quantity of semiconductors. The size and nature of specimen is independent of this technique. The FL emission properties, particularly the size of the sample can change in the nanoscale regime. It helps to determine the properties *i.e.*, structure and concentration of the emitting species, band gap, exciton lifetime, exciton energy, bi-exciton etc. [7]. This can be applied to track salvation dynamics, measure local friction, chemical reaction sensitivity, local electrical environment polarity, hydrophobicity, chemical equilibrium etc. However, energy transfer between CdS host and Pr^{3+} ions is not considered in detail in this paper. From the obtained result in the form of characterization spectra, Fourier transform infrared (IR) spectra, chromaticity diagrams and the then derived optical parameters; which will be discussed in the subsequent sections, it can be concluded that the synthesized Pr^{3+} doped CdS nanomaterials could be useful for display devices, LED, design of UV sensors, memory devices, medical, photovaltaic and optoelectronic devices. More specifically it can be utilized for temperature sensing measurement and bio-sensing detectors.

Theoretical Considerations

Radiative Properties

The radiative properties of nanoparticles are significant to the functionality as well as the performance of many devices *viz.*, radiation detectors, semiconductor lasers, solar cells, tunable optical filters, waveguides, and specific absorbers and emitters [8]. Radiative properties are fundamental physical properties that describe the interaction of electromagnetic waves with matter, ranging from ultraviolet (UV) to deep IR spectra regions. Measurement of radiative properties of a material enables us to understand the physics of powder, solid, liquid, gas and other states [9]. The radiative properties of rare earth ions have been theoretically correlated in absorption spectra with Judd-Ofelt (J-O) intensity parameters *i.e.* called as the laser parameters.

Spontaneous Emission Probability

The spontaneous emission probability (A) from an initial manifold $\left|f^N\left(\alpha',S',L'\right)J'>\right|$ to a terminal manifold $\left|f^N(\alpha,S,L)J>\right|$ is given by [10]:

$$A = \frac{64\pi^4 e^2}{3h(2J'+1)\lambda_p^3} n\left[\frac{(n^2+2)^2}{9}\right] \sum_{\lambda=2,4,6} \Omega_\lambda \left|f^N\left(\alpha',S',L'\right)J' > \left|\left|\mathrm{U}^\lambda\right|\right| f^N(\alpha,S,L)J >\right|^2 \tag{1}$$

where h is the Planck's constant and n is the refractive index.

Fluorescence Branching Ratio

The fluorescence branching ratio (β) depends on the spontaneous emission probability (A). It is the ratio of spontaneous emission probability to total spontaneous emission probability. For the transitions originating from a specific initial manifold $\left|f^N\left(\alpha',S',L'\right)J'>\right|$ it is defined as

$$\beta = \frac{A}{\sum_{\overline{\alpha SLJ}} A} \tag{2}$$

Radiative Lifetime

The radiative life time (τ) for a transition is the reciprocal of spontaneous emission probability A, for a radiative decay from the initial manifold $\left|f^N\left(\alpha',S',L'\right)J'>\right|$. It is given by [11]

$$\tau = A^{-1} \tag{3}$$

Stimulated Emission Cross-section

The stimulated emission cross-section (σ_p), for the transition from an initial manifold $\left|f^N\left(\alpha',S',L'\right)J'>\right|$ to a terminal manifold $\left|f^N(\alpha,S,L)J>\right|$ having a probability A is expressed as

$$\sigma_p = \frac{\lambda_\mathrm{p}^4}{8\pi c n^2 \Delta\lambda_\mathrm{eff}} A \tag{4}$$

where λ_p is the peak fluorescence wavelength and $\Delta\lambda_\mathrm{eff}$ is the effective line width as given by

$$\Delta\lambda_\mathrm{eff} = \frac{\int I(\lambda)d\lambda}{I_\mathrm{max}} \tag{5}$$

where $I(\lambda)$ is fluorescence intensity at wavelength λ.

In the case of absorption band, absorption of radiant energy or oscillator strength is given by [12]

$$P_{exp} = 4.6 \times 10^{-9} \times \epsilon \times \Delta\upsilon_{\frac{1}{2}} \tag{6}$$

where ϵ is the molar absorptivity of a band at a particular energy. The molar absorptivity at given energy is computed from the Beer-Lambert's law

$$\varepsilon = \frac{1}{cl(\log\frac{I_0}{I})} \tag{7}$$

where c is the molar concentration of the absorbing ion unit volume, I is the path length, $\log\frac{I_0}{I}$ is the absorptivity or optical density and $\Delta\nu_{\frac{1}{2}}$ is the half band width.

In order to choose a suitable material for laser action, it is necessary to study the various transitions giving rise to fluorescence and then compute its laser parameters utilizing the absorption and fluorescence data [13]. The laser parameters are used to predict the laser action. High value of σ_p and minimum value of A are considered to be favorable for a possible selection of suitable laser transitions.

In this paper, the various possible laser transitions in Pr^{+3} ion doped CdS nanomaterials have been computed. The various laser parameters like spontaneous emission probability (A), branching ratio (β), radiative life time (τ), and stimulated emission cross-section (σ_p) have been calculated and thereby compared with the chromaticity diagram.

Experimental Details

The CdS: Pr^{3+} nanomaterial were synthesized by simple chemical precipitation synthesis method [14]. A paper on the synthesis of CdS nanoparticles using the chemical precipitation method has been published recently by Jitendra Pal Singh et al. [15].

This is an easy, inexpensive, and single-step method. The chemicals, used in this work, were of analytical grade without purification. Cadmium nitrate tetrahydrate [$Cd(NO_3)_2.4H_2O$], sodium sulphide [Na_2S], diethylene glycol [DEG], ethanol [C_2H_5OH], praseodymium chloride [$PrCl_3$] and distilled water were used as a source material. At first 0.1M of $Cd(NO_3)_2.4H_2O$ solution (50ml) was taken in conical flask and around 20 ml of diethylene glycol (DEG) was added to this $Cd(NO_3)_2.4H_2O$ solution under constant stirring. Then 50 ml Na_2S solution and different concentration (0.1, 0.2 & 0.3 mol %) of $PrCl_3$ were added drop wise under constant stirring and it was kept for reaction for 4 hrs at 60^0C with constant stirring. Finally, a yellow precipitate of CdS is formed. It was washed with ethanol and distilled water and dried at room temperature [16]. Some portion of this dried sample is shown in Fig. 1(A) and the solutions of Pr^{3+}

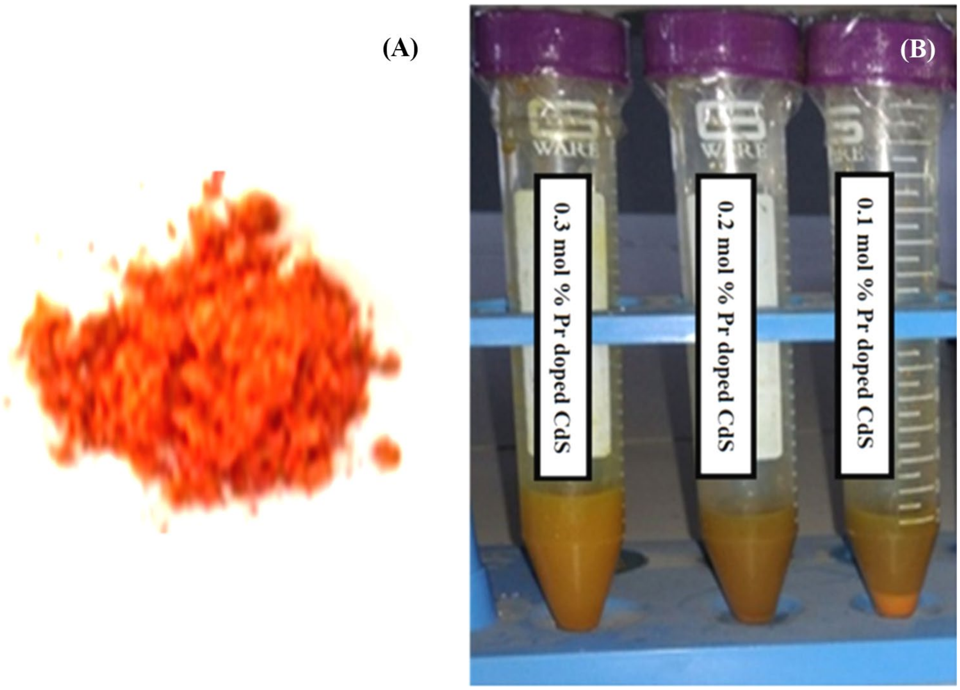

Fig. 1 (**A**) The dried powder form of CdS nanoparticles, and (**B**) the solutions of Pr^{3+} doped CdS nanoparticles of different concentrations

doped (0.1, 0.2 & 0.3 mol %) CdS nanoparticles of different concentrations are shown in Fig. 1(B).

The Scanning Electron Microscopy (SEM) images of Pr^{3+} doped CdS nanoparticles prepared by simple chemical aqueous precipitation method at room temperature is shown in Fig. 2(A), (B) and (C) respectively for 0.1 mol %, 0.2 mol % & 0.3 mol % doping concentration of Pr^{3+} ions. The images show approximate spherical shape of CdS nanoparticle and the size of the particles are around 1 μ-200 nm. It demonstrates clearly the formation of spherical CdS nanoparticles, and change of morphology of the nanoparticles with the Pr^{3+} ion concentrations. So, it can be concluded that the synthesized particles are nearly spherical shaped and the grain size is decreased with the increase of Pr^{3+} ion concentration.

The FL spectra in the spectral range of 200-900 nm and 800-1500 nm were recorded on Hitachi Model F-4600 FL spectrophotometer and Edinburgh model FLS 980 spectrophotometer respectively. The processes concerned in

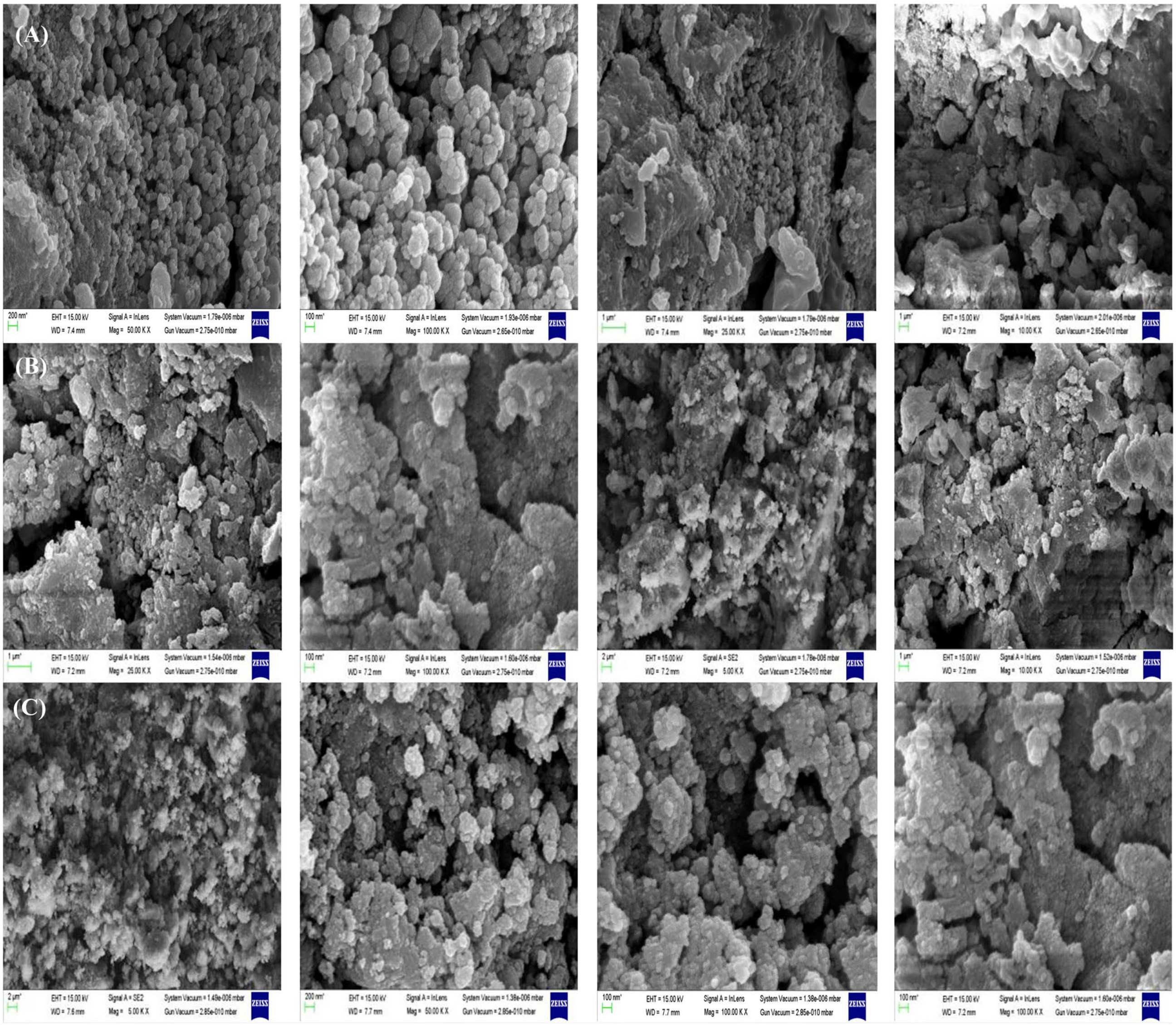

Fig. 2 SEM images of Pr^{3+} doped CdS nanoparticles prepared by simple chemical aqueous precipitation method for (**A**) 0.1 mol %, (**B**) 0.2 mol % and (**C**) 0.3 mol % doping concentration of Pr^{3+} ions at room temperature

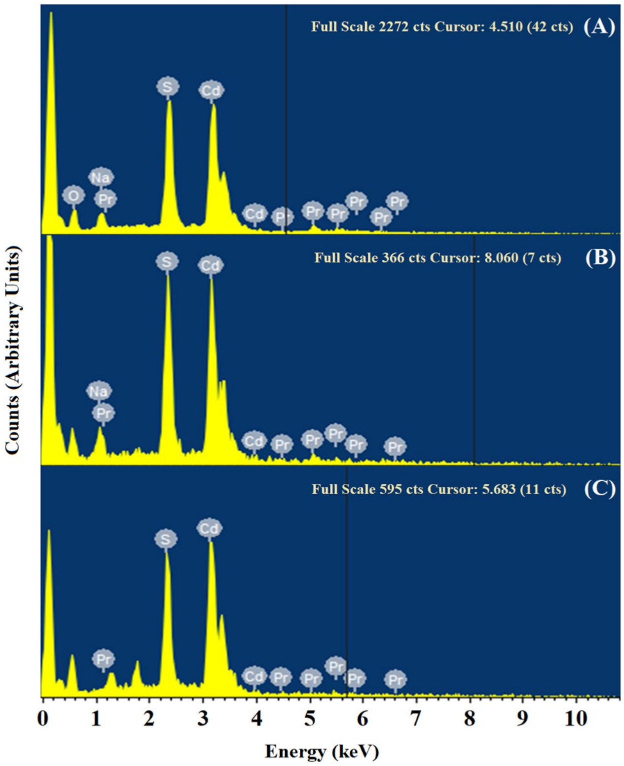

Fig. 3 EDAX spectrum of CdS nanomaterial with (**A**) 0.1 mol %, (**B**) 0.2 mol % and (**C**) 0.3 mol % doping concentration of Pr^{3+} ion

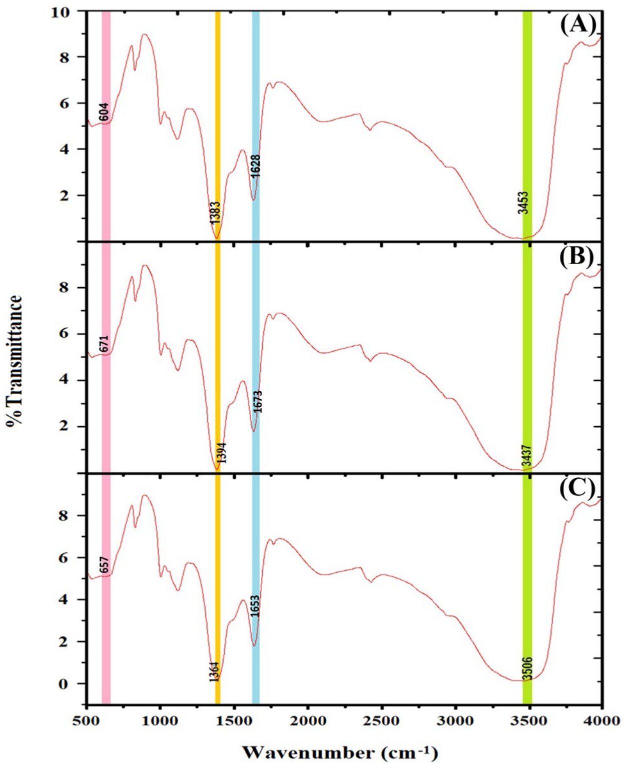

Fig. 4 FTIR spectrum of CdS nanomaterials with (**A**) 0.1 mol %, (**B**) 0.2 mol % and (**C**) 0.3 mol % of Pr^{3+} ion

Table 1 Observed band of Pr^{3+} doped CdS nanoparticles of different concentrations

S. No.	Wavenumber (cm^{-1})			Bands
	0.1% Pr^{3+} doped CdS	0.2% Pr^{3+} doped CdS	0.3% Pr^{3+} doped CdS	
1	604	671	657	Pr^{3+}/CdS
2	1383	1394	1364	S=O
3	1628	1673	1653	Cd-S
4	3453	3437	3506	O-H

absorption spectrometry are absorption and transmission based on the Lambert's law. The spectral measurements were carried out with the help of spectrophotometer method. The absorption spectra were recorded in the spectral range 300-2400 nm by Varian carry spectrophotometer. The excitation of the Pr^{3+} ions is done by the radiations (optical pumping) corresponding to its intense absorption bands.

Result and Discussion

Characterization Spectra

Repersentative energy dispersive X-ray (EDAX) spectrum of CdS nanomaterials doped with 0.1%, 0.2%, 0.3% mol

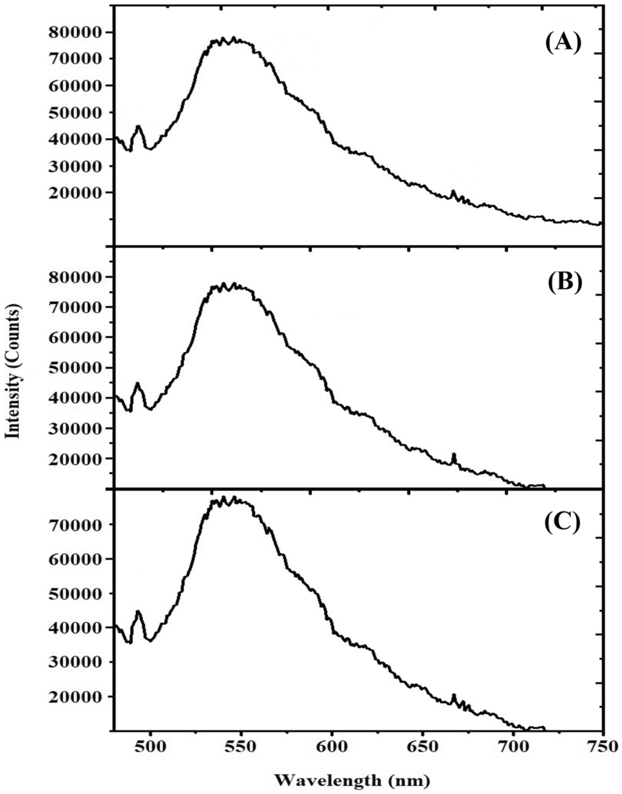

Fig. 5 Fluorescene spectrum of CdS nanomaterial with (**A**) 0.1 mol %, (**B**) 0.2 mol % and (**C**) 0.3 mol % Pr^{3+} ion

Table 2 J-O intensity parameters for Pr^{3+} doped CdS nanoparticles

Parameters	**0.1 mol % Pr^{3+}doped CdS**	**0.2 mol % Pr^{3+}doped CdS**	**0.3 mol % Pr^{3+}doped CdS**
Ω_2 (10^{-20})	1.53	3.86	0.624
Ω_4 (10^{-20})	2.32	5.86	0.17
Ω_6 (10^{-20})	7.24	3.76	0.36
Ω_4 / Ω_6	0.32	1.55	0.47
Goodness fit	27.22	75.21	411

Pr^{3+} ions has been shown shown respectively in Fig. 3(A), (B) and (C). These spectra, confirmed the chemical identity of the nanoparticles, in which the presence of Cd, S and Pr is evident.

Fourier Transform Infrared Spectroscopy

Fourier Transform Infrared (FTIR) spectrum is formed as a consequence of the absorption of the electromagnetic radiation at frequency of vibration of specific sets of chemical bands within a molecules [8]. The FTIR spectrum is obtained in the range of 500-4000 cm^{-1} and is shown in Fig. 4.

The observed band of Pr^{3+} doped CdS nanomaterials with different concentrations are given in Table 1. The presence of hydrogen and oxygen is the useful characteristic of Pr^{3+} (0.1%, 0.2%, 0.3%) doped CdS in all IR groups. The absorption peak in the range of 3201-3326 cm^{-1} could be attributed to the –OH group of water absorbed by the samples. The peak around 1628-1673 cm^{-1} is assigned to the asymmetric stretching vibration of Cd-S band from sulphur group. The peak in the range 1364-1394 cm^{-1} are due to the sulphate (S=O) group [17]. Absorption band at around 1200 cm^{-1} is due to the C-O stretching vibration of ethanol used for the synthesis [18]. The peak in the range 604-671 cm^{-1} are due to Pr^{3+} doped CdS nanoparticles [9].

In FTIR spectrum the peak at 604 cm^{-1}, 671 cm^{-1} and 657 cm^{-1} were ascribed to different concentration of Pr^{3+} doped CdS nanomaterials respectively. The bulk information on the IR spectra of CdS lies among 1628 cm^{-1}, 1653 cm^{-1} and 1673 cm^{-1}. The absorption band at about 3453 cm^{-1}, 3437 cm^{-1} and 3506 cm^{-1} was attributed to the O-H stretching vibrations in both Pr^{3+} and CdS and are originating from the surface O-H groups.

The peaks around at 1628 cm^{-1} are due to the first overtone of the fundamental stretching mode of the O-H bond [10]. The IR band among 604 cm^{-1}, 671 cm^{-1} and 657 cm^{-1} can be associated with oxygen deficiency and/or oxygen vacancy defect complex and CdS [13]. Changes of the oxygen composition can also be evaluated indirectly considering the intensity of the spectroscopic band at about 671 cm^{-1} because this vibration is caused only by the oxygen sublattice. J-O theory [19] is usually adopted to calculate the transition probabilities from the data of absorption cross-section of several f-f transitions. According to this theory, the strength of an f-f transition may be expressed by the products of three intensity parameters Ω_λ ($\lambda = 2, 4, 6$) times

Table 3 Spontaneous emission probability (A), fluorescence branching ratio (β), radiative lifetime (τ) for 0.1 mol%, 0.2 mol% and 0.3 mol% Pr^{3+} ion doped CdS nanomaterials

Transition levels	**Pr^{3+} doping concentration in CdS nanomaterial**	**Wavelength λ (nm)**	**$\Delta\lambda_{eff}$ (nm)**	**A (sec^{-1})**	**β**	**τ (μsec)**	**σ_p (10^{-18}) cm^2**
$^3P_0 \rightarrow {}^3H_4$	0.1 mol%	493	5	1808.9	0.165	552.8	3.78
	0.2 mol%	492	4	4597.0	0.283	217.5	11.91
	0.3 mol%	494	5	131.4	0.041	7590	0.27
$^3P_1 \rightarrow {}^3H_6$	0.1 mol%	546	51	1761.2	0.160	567.7	0.54
$^3P_0 \rightarrow {}^3H_6$				1508.2	0.137	663.0	0.46
$^1D_2 \rightarrow {}^3H_4$				3022.7	0.275	330.8	0.93
$^3P_1 \rightarrow {}^3F_2$				1334.5	0.121	749.3	0.41
$^3P_1 \rightarrow {}^3H_6$	0.2 mol%	546	51	914.68	0.056	1093.2	0.28
$^3P_0 \rightarrow {}^3H_6$				3805.1	0.234	262.79	1.17
$^1D_2 \rightarrow {}^3H_4$				1569.8	0.096	637.01	0.48
$^3P_1 \rightarrow {}^3F_2$				1468.2	0.090	681.09	0.45
$^3P_1 \rightarrow {}^3H_6$	0.3 mol%	546	50	89.27	0.028	1120	0.028
$^3P_0 \rightarrow {}^3H_6$				615.13	0.19	1625	0.19
$^1D_2 \rightarrow {}^3H_4$				153.22	0.048	6526	0.048
$^3P_1 \rightarrow {}^3F_2$				1546.5	0.48	646.5	0.48
$^3P_0 \rightarrow {}^3F_2$	0.1 mol%	668	3	1521.6	0.138	657.2	0.46
	0.2 mol%	667	4	3838.8	0.237	260.4	1.18
	0.3 mol%	669	2	620.57	0.196	1611	0.19

Table 4 Comparative study of stimulated emission cross-section in Pr^{3+} doped CdS nanomaterial

Sample Material	Wavelength (nm)	σ_p (cm^2) (${}^3P_0 \rightarrow {}^3H_4$)	Reference
Pr^{3+}doped CdS (0.1 mol%)	493	3.78 (10^{-18})	Present work
Pr^{3+}doped CdS (0.2 mol%)	492	11.91 (10^{-18})	Present work
Pr^{3+}doped CdS (0.3 mol%)	494	0.27 (10^{-18})	Present work
Pr^{3+} doped borosilicate glasses (BSGPR02)	492	2.58 (10^{-18})	[21]
Pr^{3+} doped borosilicate (BSGPR16)	492	3.29 (10^{-18})	[21]
Borosilicate glass with 0.5% of Pr^{3+}	490	3.84 (10^{-20})	[22]
Pr^{3+} doped Zinc oxide (0.1 mol%)	445	2.98 (10^{-20})	[23]
Pr^{3+} doped Zinc oxide (0.2 mol%)	445	3.36 (10^{-20})	[23]
Pr^{3+} doped Zinc oxide (0.3 mol%)	445	1.35(10^{-20})	[23]

the squared matrix element U^λ between the initial J-states and the terminal $J^{'}$-state. Once the phenomenological parameter Ω_λ have been calculated, it is possible to derive the strength of any absorption or emission transition, as well as the stimulated emission cross-section, the fluorescence branching ratio from level J to $J^{'}$. It is also useful to calculate the radiative lifetime of an excited level. The luminescent properties of rare earth ions are necessary to know their key energy levels. The FL spectra of CdS nanomaterial with 0.1 mol %, 0.2 mol % and 0.3 mol % doping of Pr^{3+} ions is shown in Fig. 5 which is indicating the comparative study of ${}^3P_0 \rightarrow {}^3H_4$, ${}^3P_1 \rightarrow {}^3H_6$, ${}^3P_0 \rightarrow {}^3H_6$, ${}^1D_2 \rightarrow {}^3H_4$, ${}^3P_1 \rightarrow {}^3F_2$ and ${}^3P_0 \rightarrow {}^3F_2$ transitions for 0.1 mol%, 0.2 mol% and 0.3 mol% Pr^{3+} ion doped CdS nanomaterial samples in Fig. 5(A), (B) and (C) respectively.

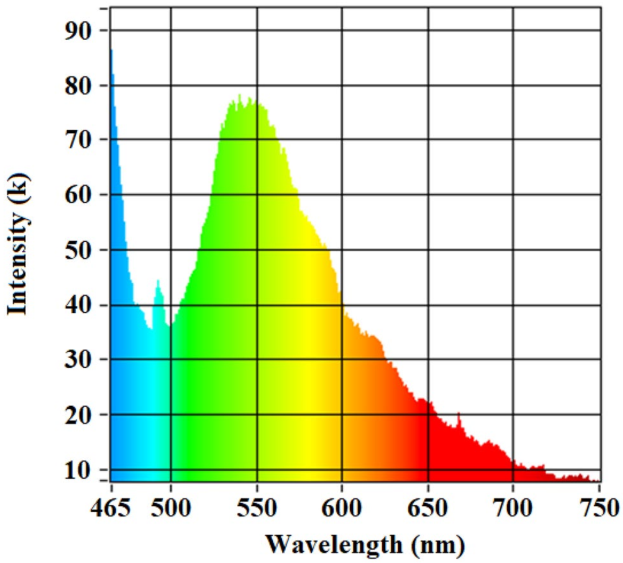

Fig. 7 Spectral graph of CIE chromaticity diagram for CdS doped Pr^{+3} Specimen

Table 2 shows the J-O intensity parameters, for Pr^{3+} doped CdS nanoparticles, which was calculated by using the absorption spectra of the synthesized nanoparticles [20].

The various laser parameters like spontaneous emission probability (A), branching ratio (β), radiative life time (τ), and stimulated emission cross-section (σ_p) have been calculated by using the fluorescence wavelength matrix elements for relevant transitions and J-O parameters. The results were obtained

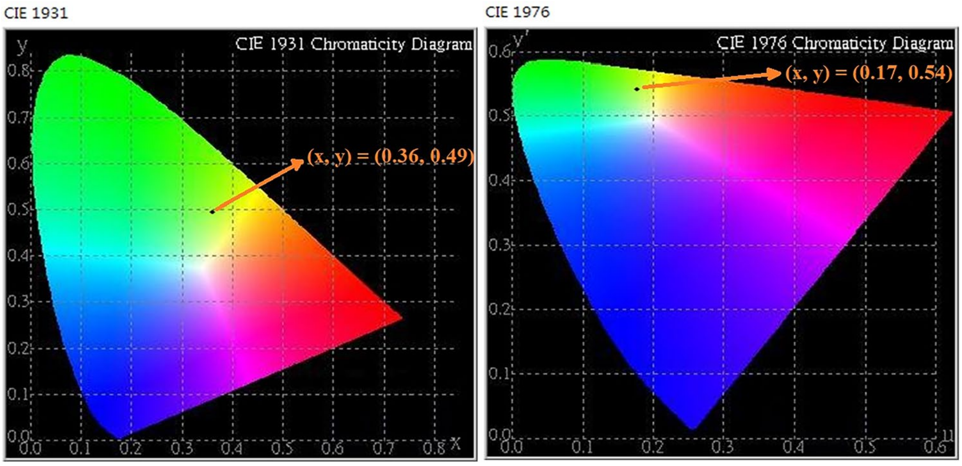

Fig. 6 CIE chromaticity diagram

Table 5 Optical parameters of the prepared Pr^{3+}doped CdS nanoparticles

Pr^{3+} doping concentration in CdS nanomaterial	Refractive index	Dielectric Constant	Optical dielectric Constant	Reflection losses
0.1 mol %	1.574	2.477	1.477	0.0492
0.2 mol %	1.585	2.512	1.512	0.0506
0.3 mol %	1.589	2.524	1.524	0.0515

for 0.1 mol%, 0.2 mol% and 0.3 mol% Pr^{3+} ion doped CdS nanomaterial samples and is given in Table 3. These results are further compared with the chromaticity diagram.

In the used Pr^{3+} doped CdS nanomaterial sample most intense band in the absorption spectra around 423 nm ($^3P_0 \rightarrow {}^3H_4$) has been used for the excitation. As a consequence of this, three fluorescence band around 493 nm, 546 nm and 668 nm for 0.1 mol % Pr^{3+} doped CdS, three fluorescence band around 493 nm, 546 nm and 668 nm for 0.2 mol % Pr^{3+} doped CdS and three fluorescence band around 492 nm, 546 nm and 667 nm for 0.3 mol % Pr^{3+} doped CdS have been observed. They have been assigned to the transition $^3P_0 \rightarrow {}^3H_{4,}$ $^3P_1 \rightarrow {}^3H_{6,}$ $^3P_0 \rightarrow {}^3H_{6,}$ $^1D_2 \rightarrow {}^3H_4$,$^3P_1 \rightarrow {}^3F_2$ and $^3P_0 \rightarrow {}^3F_2$ respectively.

In Table 4 a comparative study of stimulated emission cross-section in Pr^{3+} doped CdS nanomaterial is given. The stimulated emission cross-section is an important laser parameter and its value signifies the rate of energy extraction from the laser material prepared in laboratory scale. The high value of σ_p for $^3P_0 \rightarrow {}^3H_4$ transition is identifying this as the potential laser transition. This transition can be used as low threshold and high gain laser applications. It is clear from Table 4, that the value of A is maximum for the $^3P_0 \rightarrow {}^3H_4$ transition for all the cases of considered Pr^{3+} doped CdS nanomaterials. This gives the suitability of this transition for laser action in visible region. In case of the considered Pr^{3+} doped CdS nanomaterial, the Pr^{3+} ion gives blue emission.

CIE Chromaticity Diagrams

For the measuring of the coulor of visible emission that can be perceived by the human eye the Commision Internationale de l'Eclariage (CIE) coordinates were calculated. It is a standard method for defining the colour and is obtained by considering the sensitivity of human eye for different colours and wavelengths [24, 25]. There are two methods for recording the chromaticity diagram *viz.*, CIE1931 and CIE1976.

Figure 6 represents these CIE chromaticity diagram for 0.2 mol % Pr^{3+} ion doped CdS nanoparticles. This diagram was obtained from the FL spectra data. The CIE coordinates for the Pr^{3+} doped CdS nanoparticles by both the methods shows that the chromaticity coordinates lies in the blue region of this diagram. As Pr^{3+} doped glasses give blue emission, it is obtained for the present glass samples. CIE chromaticity diagram verifies the result of fluorescence. The spectral graph clearly shows that the emission colour for Pr^{3+} doped CdS nanomaterial is in the blue region and it also verifies the result of fluorescence showing that the most probable transition is at 493 nm (Fig. 7).

Optical Parameters

Different optical parameters like refractive index (n), dielectric constant (ε), optical dielectric constant (ε_o), molar volume (V_m), reflection losses (R) of the synthesized Pr^{3+} doped CdS nanoparticle specimens were computed and presented in Table 5.

Conclusion

We have successfully prepared Pr^{3+}doped CdS nanoparticles by simple chemical precipitated method with an objective to use them as fluorescence laser. The chemical identity of the nanoparticles was confirmed by EDAX spectrum and the absorption peaks was confirmed by the FTIR spectrum. The SEM images clearly signifying the change of morphology of the spherical CdS nanoparticles with the Pr^{3+} ion doping concentrations. In Pr^{3+} doped CdS nanomaterial, the J-O intensity parameter, the radiative rates, the branching ratio and the fluorescence lifetime were calculated from the experimental absorption emission spectrum. The result shows that both down-conversion and up-conversion photoluminescence of Pr^{3+} doped CdS nanoparticles were significantly dependent on concentration of CdS nanoparticles and annealing temperature. The spectral chromaticity diagram clearly shows that the emission colour for Pr^{3+} doped CdS nanomaterial is in the blue region and it also verifies the result of fluorescence showing that the most probable transition is at 493 nm. The comparative study of stimulated emission cross-section corresponding to the $^3P_0 \rightarrow {}^3H_4$ transition in Pr^{3+} doped CdS nanomaterial, confirms the suitability of the observed $^3P_0 \rightarrow {}^3H_4$ transition for laser action in visible region. From the above result we deduce that CdS nanoparticles enter the glass as a network modifier, increase the number of non-bridging oxygen in the glass network and weaken the Si-O bonds. The developed Pr^{3+} doped CdS nanoparticles could be useful for display devices, LED, design of UV Sensors for temperature measurement [26] and biosensors [27], memory devices, medical, photovaltaic and optoelectronic devices.

Acknowledgement Acknowledgements are due to Institute Instrumentation Centre (IIC), IIT Roorkee for providing facilities for recording FL spectra and absorption spectra of the sample. Thanks are due to Prof. Ramesh Chandra, Head, IIC, IIT Roorkee for his valuable help in this study.

Authors' Contributions Jitendra Pal Singh and Sudha Pal take the data, Yogesh Kumar Sharma wrote the main manuscript text, Atanu Nag prepared Figs. 2, 3, 4. All authors reviewed the manuscript.

Availability of Data and Materials The datasets used and/or analysed during the current study are all available in the manuscript in details, for more information contact the corresponding author.

Declarations

Ethical Approval Not Applicable.

Conflict of Interests The authors have no relevant financial or non-financial interests to disclose.

References

1. Xuemin Q, Huibiao L, Yanbing G, Shigun Z, Yinglin S, Yinglin S, Yuliang L (2009) Field Emission Properties and fabrication of CdS Nanotube arrays. Nanoscale Res Lett 4:955–961
2. Shen SG, Chen X, Ren F, Mao SS (2010) Effect of Ag_2S on Solar-Driven Photocatalytic Hydrogen Evolution of Nanostructured CdS. Int J Hydrog Energy 35:7110–7115
3. Rajvee R, Prabhu M, Khadar A (2005) Characterization of chemically synthesized CdS Nanoparticles. Pramana J Phys 65:801–807
4. Patel NH (2015) Preparation Characterization of undoped and doped CdS Nanoparticles. Dissertation, Sardar Patel University
5. Hugues L, Benoit C (2016) Spectroscopic studies of Neodymium and Praseodymium compounds in molten chlorides. Sci Direct Procedia Chem 21:409–416
6. Kumar NS, Govinda D, Rao GT (2017) Synthesis, structural and morphological studies of CdS Nanopowder. Int J Chem Sci 14(1):409–414
7. Bishnoi NB, Sharma YK, Surana SSL, Tandon SP (1993) Electrical and optical study of Cr^{3+} doped chlorophosphate and phosphate glasses. Synth Met 55:469–474
8. Zhang ZM (2020) Radiative Properties of Nanomaterials. In: Nano/Microscale Heat Transfer, Mechanical Engineering Series, Springer, Cham. https://doi.org/10.1007/978-3-030-45039-7_9
9. Ravindra NM, Marthi SR, Bañobre A (2017) Radiative properties of semiconductors. Morgan and Claypool Publishers
10. Surana SSL, Gehlot CL, Tandon SP, Sharma YK (2003) Fluorescence of Sm^{3+}, Eu^{3+}, Ho^{3+} and Er^{3+} doped Borophosphate glasses. Can J Anal Sci Spectrosc 48:285–294
11. Bokatial L, Rai S (2010) Optical properties and up-conversion of Pr3 + doped CdS nanoparticles in sol–gel glasses. J Lumin 130:1857–1862
12. Mehta PC, Tandon SP (1970) Spectral intensities of some Nd^{3+} β-diketonates. J Chem Phys 53:41
13. Sharma YK, Goyal P, Pal S, Bind UC (2016) Laser action in Praseodymium Doped Borosilicate Glasses in visible region. J Chem Eng Chem Res 3:1031–1035
14. Sahare P (2018) Synthesis and characterization of CdS nanoparticle. Int J Eng Res Technol 6:2278–2281
15. Singh JP, Goyal P, Sharma YK, Prakash DR (2019) Synthesis and characterization of Pr^{3+} doped CdS nanomaterial. J Emerg Technol Innovative Res 6:3093–3101
16. Saravanan L, Jayavel R, Pandurangan A, Liu JH, Yuan MH (2014) Synthesis structural and optical properties of $Sm^{+\,3}$ and Nd^{3+} doped Cadmium Sulfide nanocystals. Mater Res Bull 52:128–133
17. Sabah A, Siddiqi SA, Ali S (2010) Fabrication and Characterization of CdS Nanoparticles Annealed by using Different Radiations. World Acad Sci Eng Technol 69:82–89
18. Rao BS, Kumar BR, Reddy VR, Rao TS (2011) Preparation and characterization of CdS nanoparticles by chemical co-precipitation technique. Chalcogenide Lett 8:177–185
19. Goyal P, Sharma YK, Pal S, Bind UC, Huang S, Chang S (2017) The effect of SiO_2 content on Structural, Physical and Spectroscopic properties of Er^{3+}doped B_2O_3-SiO_2-Na_2O-PbO-ZnO glass system. J Non-cryst Solids 463:118–127
20. Singh JP, Goyal P, Sharma YK, Kumar V (2021) Optical energy band gap and absorption spectra of CdS:Pr^{3+} nanomaterials. Int J Curr Adv Res 10:24429–24432
21. Sharma YK, Surana SSL, Singh RK (2014) Optical absorption and fluorescence spectra of Pr^{3+} doped borosilicate glasses and their Judd-Ofelt analysis to study lasing characteristics. Indian J Eng and Science 4:17–24
22. Sharma YK, Joshi RP, Pal S, Goyal P (2016) Spectroscopic Properties of lithium Borate Glass Material with Neodymium ions. Chiang. Mai J Sci 43:311–319
23. Pal S, Sharma YK, Singh JP (2021) Spectra:Structral and characterization of Neodymium ions doped Zine Oxide Nanomaterial. Am J Nanosciences 7:49–53
24. Hao N, Nie Y, Xu Z, Jin C, Fyda TJ, Zhang JXJ (2020) Microfluidics-enabled acceleration of Fenton oxidation for degradation of organic dyes with rod-like zero-valent iron nanoassemblies. J Colloid interface Sci 559:254–262
25. Singh A, Ahmed A, Sharma A, Sharma C, Paul S, Khosla A, Gupta V, Arya S (2021) Promising photocatalytic degradation of methyl orange dye via sol-gel synthesized Ag-CdS@Pr-TiO_2 Core /shell nanoparticles. Physica B 612:413121
26. Zhou S, Jiang G, Wei X, Duan CK (2014) Pr^{3+}-Doped beta-NaYF4 for temperature sensing with fluorescence intensity ratio technique. J Nanosci Nanotechnol 14:3739–3742
27. Zhang J, Chen H, Xu K, Deng D, Zhang Q, Luo L (2023) Current progress of ratiometric fluorescence sensors based on Carbon Dots in Foodborne Contaminant Detection. Biosensors 13:233